

This article was downloaded by:

On: 23 January 2011

Access details: *Access Details: Free Access*

Publisher *Taylor & Francis*

Informa Ltd Registered in England and Wales Registered Number: 1072954 Registered office: Mortimer House, 37-41 Mortimer Street, London W1T 3JH, UK



## Journal of Coordination Chemistry

Publication details, including instructions for authors and subscription information:

<http://www.informaworld.com/smpp/title~content=t713455674>

### INFLUENCE OF THE SOLVENT IN THE ELECTRONIC SPECTRA OF AZABIPYRIDINE MACROCYCLES OF ZINC(II) AND NICKEL(II)

G. Estiu<sup>a</sup>; J. Canales<sup>b</sup>; J. Ramirez<sup>b</sup>; J. Costamagna<sup>b</sup>

<sup>a</sup> CEQUINOR, Faculty of Exact Sciences, Universidad Nacional de La Plata, La Plata, Argentina <sup>b</sup> Faculty of Chemistry and Biology, Universidad de Santiago de Chile, Santiago-33, Chile

**To cite this Article** Estiu, G. , Canales, J. , Ramirez, J. and Costamagna, J.(2001) 'INFLUENCE OF THE SOLVENT IN THE ELECTRONIC SPECTRA OF AZABIPYRIDINE MACROCYCLES OF ZINC(II) AND NICKEL(II)', *Journal of Coordination Chemistry*, 54: 3, 193 – 214

**To link to this Article:** DOI: 10.1080/00958970108022635

**URL:** <http://dx.doi.org/10.1080/00958970108022635>

PLEASE SCROLL DOWN FOR ARTICLE

Full terms and conditions of use: <http://www.informaworld.com/terms-and-conditions-of-access.pdf>

This article may be used for research, teaching and private study purposes. Any substantial or systematic reproduction, re-distribution, re-selling, loan or sub-licensing, systematic supply or distribution in any form to anyone is expressly forbidden.

The publisher does not give any warranty express or implied or make any representation that the contents will be complete or accurate or up to date. The accuracy of any instructions, formulae and drug doses should be independently verified with primary sources. The publisher shall not be liable for any loss, actions, claims, proceedings, demand or costs or damages whatsoever or howsoever caused arising directly or indirectly in connection with or arising out of the use of this material.

# INFLUENCE OF THE SOLVENT IN THE ELECTRONIC SPECTRA OF AZABIPYRIDINE MACROCYCLES OF ZINC(II) AND NICKEL(II)

G. ESTIU<sup>a,\*</sup>, J. CANALES<sup>b</sup>, J. RAMIREZ<sup>b</sup>  
and J. COSTAMAGNA<sup>b,†</sup>

<sup>a</sup>*CEQUINOR, Faculty of Exact Sciences, Universidad Nacional de La Plata,  
CC 962, CP 1900, La Plata, Argentina;* <sup>b</sup>*Faculty of Chemistry and Biology,  
Universidad de Santiago de Chile, Santiago-33, Chile*

*(Received 21 August 2000; In final form 28 February 2001)*

The influence of the media on structural characteristics of bis-azabipyridil macrocyclic ligands and their Zn and Ni complexes is analyzed by means of quantum chemical calculations applied to the interpretation of UV-visible spectra. Metallic and metal-free species are considered as case studies, focusing on the influence of both coordinating and non-coordinating effects of the solvents on the structural and electronic characteristics of the systems.

Whereas cationic structures are necessary to model a protic environment, isolated molecules are not capable of rendering a good description in a non-polar environment, where intermolecular interactions are to be considered.

**Keywords:** Bis-azabipyridine macrocycles; Electronic spectroscopy; Quantum chemical calculations

## INTRODUCTION

The influence of the external environment on the chemical behavior of a system has been a matter of concern since the early days of chemical research [1].

In the case of large systems, like enzymes, metal surfaces or polymers, where only a small part is responsible for the activity, the environment is

---

\*Corresponding author. Fax: 54 221 42594, e-mail: estiu@nahuel.biol.unlp.edu.ar

†e-mail: jcostama@lauca.usach.cl

partially self-defined. Most of the effort during the last decades has been devoted to properly choosing a representative portion for modeling, which should be, at the same time, capable of avoiding “border effects”. Small molecules, on the other hand, have been treated as “complete systems” in a first approach. However, this approach is only valid when either gas phase or low concentrations of a solute in non-polar media are modeled. The incompleteness of the definition of a system by itself has demonstrated its relevance, and several ways of modeling the environment, even for small systems, have been developed, defining an area which is largely known as the treatment of solvent effects [2].

The dependence of the reactivity of a system on the surrounding media provides, in some cases, a way to handle external control on it [3,4]. The theoretical analysis of reactivity cannot disregard, thence, the incorporation of solvent effects into the quantum chemical calculations. Different approaches have been developed, which are presently mostly used in a combined fashion.

The first approaches were based in continuum models. The solvent was treated as a dielectric which is polarized by the solute charges, generating a reaction field that defines a perturbation in the Hamiltonian of the solute [2]. The continuum models have the advantage of effectively modeling the long-range electrostatic contributions. However, specific interactions between solute and solvent are not considered within this approach. In many cases, it is essential to include these interactions explicitly [5,6]; when a reaction occurs in a protic media, specific protonation of the solute, or H-bond interactions between solute and solvent, not only affect the electronic distribution, but also the geometry of the reactants. Due to this fact, discrete models have been developed, where all the interacting species are specifically defined, at the cost of increasing the size of the system and the computational cost of the calculations [7,8]. The most recent combined Quantum Mechanics/Molecular Mechanics approaches successfully deal with this problem, partitioning the system into a QM region and a MM one, the latter containing most of the information of the surroundings [9–11]. ONIOM methodologies [12,13] allow any combination of strategies of different accuracy, and are presently applied for the treatment of any kind of extended systems.

Solvent effects can be experimentally traced through the determination of physical characterization patterns, as UV-vis spectra, following their changes in response to modifications of the characteristics of the media [14–16]. Within a theoretical calculation oriented to understand this effect, an accurate reproduction of the spectra would be only compatible with an appropriate modeling of the environment, defined, in several cases, by

interacting solvent molecules [7, 17]. A large number of examples can be found in the literature, mainly related to coordination chemistry. Perhaps one of the most demonstrative examples is given by the influence of the solvent on the energy associated with LMCT transitions, which can even revert to MLCT according to the polarity of the media [18]. When the UV-vis spectrum defines the target, the most successful theoretical treatments have been achieved after the application of ZINDO/S methodologies [19, 20], an effort that should acknowledge Zerner and his collaborators.

We have centered our research in the study of the UV-vis spectra of bis-bipyridine hexa-aza-macrocyclic ligands and their Zn(II) and Ni(II) complexes, largely pH-dependent, and have applied a ZINDO/S methodology [21] at a configuration interaction (CI) level as a way to understand their chemical behavior in solution. These complexes play an important role in the activation of small molecules, like carbon dioxide, lowering its high reduction potential through electrocatalytic coordination [22–24].

Calculations are capable of reproducing the observed electronic spectra in different environments, and help to identify, in this way, the structural and electronic characteristics of the system in protic and non-protic solvents. Understanding this behavior might help to understand how the catalytic properties are influenced by the media.

## COMPUTATIONAL DETAILS

### Structural Models

Crystallographic data are not available for neither the ligand, or the coordination complexes. The first step of the study implies, then, a full geometry optimization of the structures to be analyzed. Optimization is based on a minimization of the gradient, calculated analytically, using the BFGS algorithm to update the Hessian matrix in successive geometry cycles. PM3 and AM1 Hamiltonians [25] have been compared for the ligand and the Zn complex, as they are known to have a better performance than ZINDO/1 in the optimization step [26]. Only PM3 calculations have been used to optimize the geometry of the Ni complex, as no parameters for Ni are available at the AM1 level. All self consistent field (SCF) calculations were of the restricted Hartree Fock (RHF) type.

The influence of the solvent has been treated specifically, considering the effect of protonation as well as the coordination of counterions in protic media. Tautomer species that can coexist in equilibria have been considered

for the ligand, in their neutral and protonated forms (Fig. 1), in order to model the effect of protic and aprotic environments. Single protonation has also been considered for the metal complexes, as a model for the species that can be stabilized by monoprotic counterions. When dealing with aprotic solvents, non-covalent interactions have been considered to model the environment, implying either H-bond for solvent-solute or  $\pi$ -stacking for inter-solute interactions, respectively.

### Electronic Structure Calculations

For the optimized structures, the electronic characteristics and the UV-vis spectra have been examined by means of the INDO/S methodology,

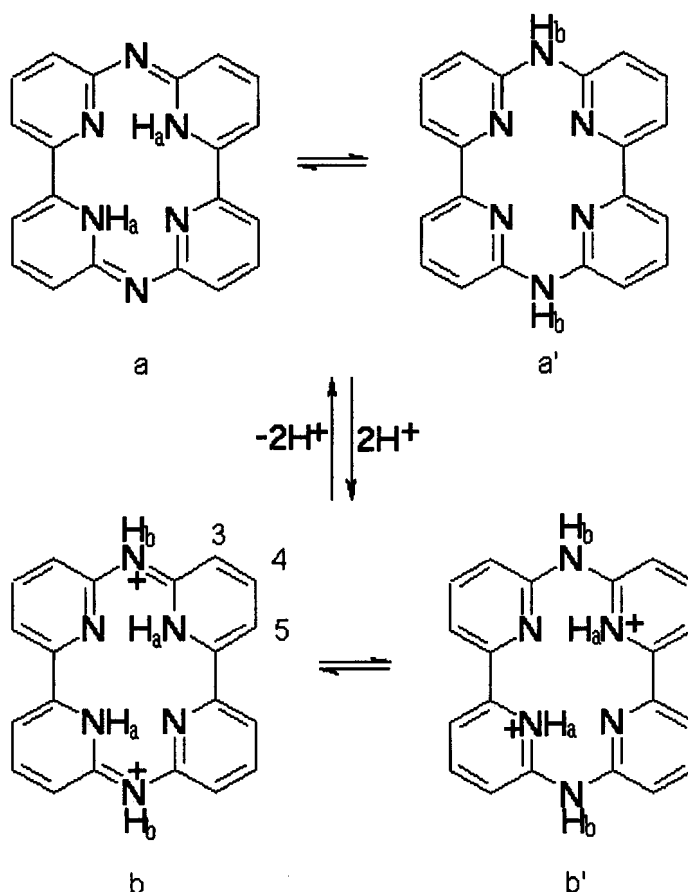


FIGURE 1 Imine (1-a, 1-b) and amine (1-a', 1-b') tautomers of the bis-azabipyridyl ligand in aprotic and protic media.

parametrized for spectroscopy [19,20], at the configuration interaction single (CIS) level of theory (ZINDO/S-CI) [21]. Several different CI calculations have been performed.

As for the geometry optimization step, tautomeric and protonated structures were analyzed for the ligand. The feasibility of the different structures has been decided on the basis of the best reproduction of the experimental spectra. Aimed by this objective, not only monomers, but also more extended systems have been considered in order to model the different experimental situations.

The same consideration has been applied for the treatment of the metal complexes. In this case, bridge aza-nitrogen protonation and counterion coordination has been used to model the protic environment.

A number of configurations larger than 1200 have been included in the CI calculations, which were generated by single electronic excitations from the upper 60 occupied to the lower 15 virtual orbitals, in both monomer and dimer compounds. This pattern was kept constant regardless the size of the system. The orbital space has been selected to include all the  $n$ , and all the  $n$  and the  $d$  orbitals, for the ligand and the complexes, respectively. The nature of the molecular orbitals (MO) involved in the excitations has been assigned on the basis of the contribution of the atomic orbitals in the linear combinations that define the MOs between which the transition occurs. Oscillator strengths were evaluated with the dipole-length operator [27], retaining all one-center terms.  $C_{2v}$  symmetry has been defined for the calculations whenever it applies.

For the ligand and the metal complexes the UV-vis spectra in chloroform and acetic acid solutions were recorded on a Varian Cary 1E spectrophotometer. Zinc and nickel elemental analyses were performed in a Perkin Elmer 2380 atomic absorption spectrophotometer, and carbon, nitrogen and hydrogen elemental analyses in a Fisons EA 1108 apparatus. Melting points were registered in an Electrothermal IA9000 apparatus. All compounds have been previously characterized as reported in Ref. [28].

## RESULTS AND DISCUSSION

### Structural Characteristics

#### *Bis-azabipy Ligands*

The tautomeric structures that can coexist in equilibrium in aprotic and protic media are shown in Figure 1. Following previous publications [29–31] we will name them imine (1-a, 1-b) and amine (1-a', 1-b') tautomers.

### (a) Aprotic Environment

Different optimized geometries result from PM3 and AM1 calculations for the deprotonated imine structure. Whereas PM3 stabilizes a completely planar structure, AM1 favors a bent one that minimizes the repulsion between the H atoms bonded to the inner nitrogens (Fig. 2). This result is a consequence of the different parametrization used for the treatment of the hydrogen bond at both levels of calculation. The stabilization of H bonds between adjacent N-atoms define a more extended delocalized  $\pi$ -system which is responsible for planarity. Due to the small energy difference between planar and bent structures, both of them have been considered for the calculation of the UV-vis spectrum.

As a way of modeling the environment, intermolecular interactions between the molecules have been considered in aprotic media. The model is defined by two ligand molecules in a parallel arrangement (see Fig. 3a) that allows their mutual stabilization by  $\pi$ -interactions.

The role of non-covalent interactions between aromatic moieties has been studied, as they influence the stability of nucleic acids [32], proteins [33], porphyrins and phthalocyanines, among others [34]. Because of the weak nature of the interactions, correlated *ab-initio* calculations with split basis

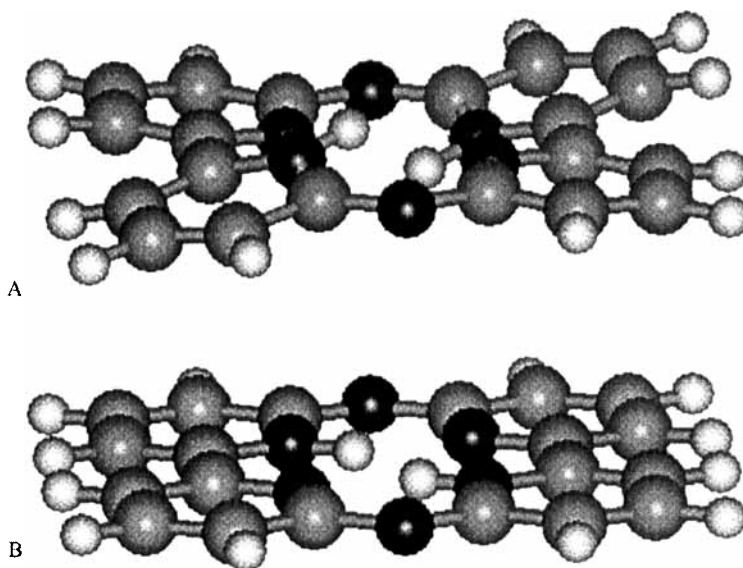


FIGURE 2 Structural characteristics of the bis-azabipyridyl ligand (imine tautomer) as result from AM1 (A) and PM3 (B) geometry optimizations. More details in the text.

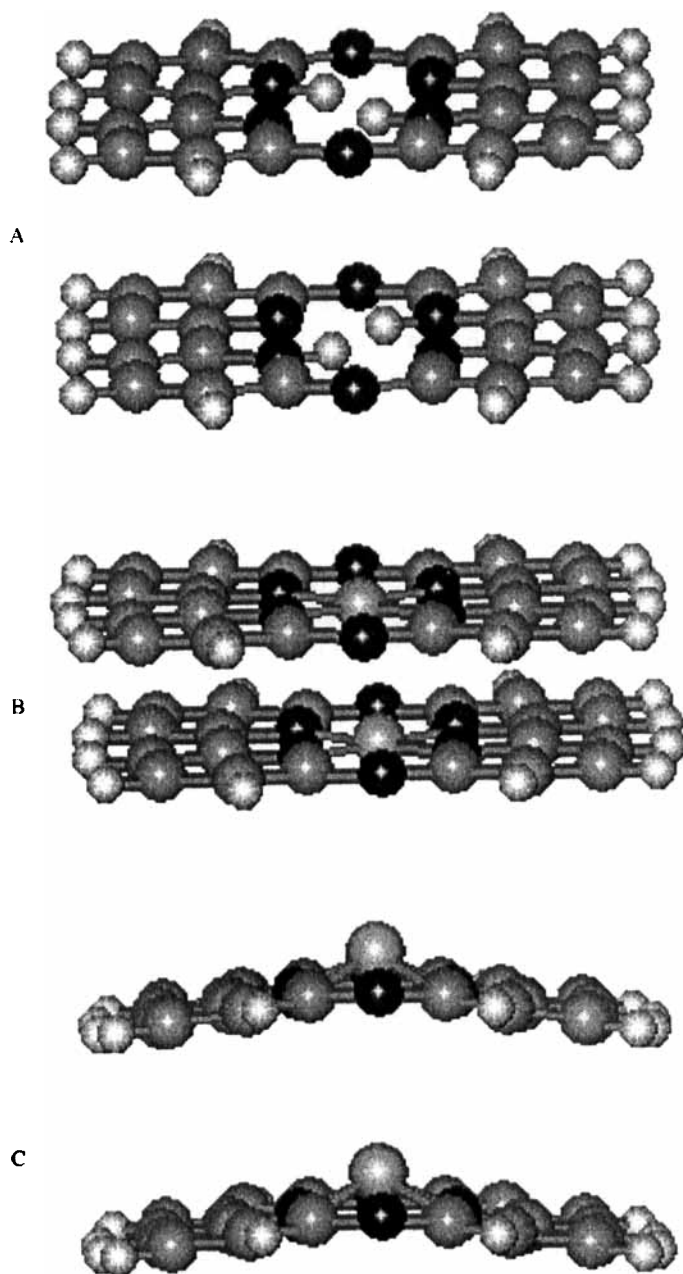


FIGURE 3 Dimeric structures for: (A) bis-azabipyridyl ligand, (B) nickel complex, (C) zinc complex used to calculate the spectra reported in Tables I, III, IV. Monomer moieties belongs to PM3 calculations. The distance between them has been chosen on the basis of the best fit of the calculated UV-vis spectra to the experimental data. More details in the text.



including polarization define the minimum requirements for their proper computational modeling [35]. Semiempirical calculations are not parametrized for weak interactions and a geometry optimization at this level led to the separation of the system in two monomeric units. Molecular mechanic force fields include non-bonded interactions in the van der Waals and electrostatic energy terms. They simulate the “staking” stabilization between aromatic rings with a precision that compares to the *ab-initio* one [35].

We have preferred to use, for our calculations, the experimental information provided by the low energy features of the UV-vis spectrum, and adjust the distance between the moieties until best fitting of the ZINDO/S-CI calculated spectrum to the experimental data. This procedure has been extensively tested [36, 37], and its credibility is, nowadays, widely accepted. As will be further discussed, a dimer built on the PM3 stabilized planar structure, with an interplanar separation of 3.3 Å between the monomers, defines the best model of the azamacrocycle ligand in non-protic media. This distance is in agreement with the one derived from molecular mechanics calculations, and close to the one calculated for toluene dimers [34a] and aza-phenanthroline macrocycles [34b]. The same interplanar distance gives the closest agreement to the experimental spectrum for the bent AM1 derived structure, but the results are less accurate than those calculated with the planar one.

### (b) Protic Environment

Protonation of the ligands has been considered (Fig 1.b, 1.b') as a way of modeling the effect of a protic environment. Figure 4 shows that no planarity is associated with the amine tautomer, in either the non-protonated form or after protonation of the inner nitrogen atoms. The

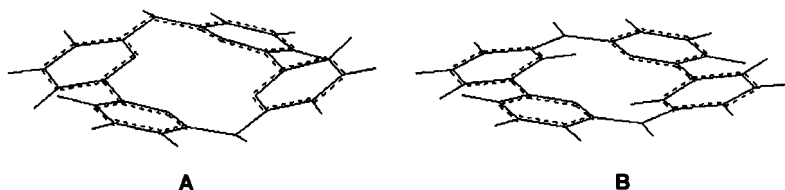


FIGURE 4 Calculated structural characteristics of the bis-azabipyridyl ligand (amine tautomer) in: (A) aprotic media, (B) protic media; related to Figure 1, a' and b', respectively. 1.b and 1.b' render the same structure after optimization. Similar structures result, in both cases, from either PM3 or AM1 calculations. PM3 results are shown.

stabilized geometry is the result of the influence of the protonated aza bridge on the torsional angle defined by the pyridine rings, which is distorted from the value characteristic of biphenyl structures. Both effects converge to a NCCN angle close to  $20^\circ$ . Results are coincident for PM3 and AM1 calculations.

### *Zn(II) and Ni(II) Complexes*

Aza-bipyridine complexes are stabilized by coordination of the Zn(II) or Ni(II) cations, which replace the inner protons of the macrocyclic ligand, (Fig. 1a), rendering a neutral complex characterized by large electronic delocalization [28].

#### *(a) Aprotic Environment*

The structure of the zinc complex is slightly distorted from planarity in the orientation of the rings, an effect originated in the position of the metal ion, which defines, with the coordinating nitrogen atoms, a square-based pyramidal structure (Fig. 3c). The same result is attained when either PM3 or AM1 calculations are performed.

A planar structure is calculated, on the other hand, for the nickel complex (Fig. 3b), as the smaller size of the Ni(II) ion is compatible with the size of the cavity defined by the coordinating nitrogen atoms.

In both cases dimeric structures have been also considered, as the aromatic delocalized system is not only characteristic of the ligand, but also of the metal complexes.

#### *(b) Protic Environment*

The interaction of a protic environment with the metal complexes has been modeled at different levels. The structures that result from PM3 calculations for one or two protonated bridge aza-nitrogens are shown in Figure 5. Similar structures are derived from AM1 calculations. Monoprotonation has been considered because it is the structure that can be stabilized by a counterion, the latter coordinating the central metal atom. Further consideration of the counterions which, within the model, stabilizes the positively charged protonated species, render the structures shown in Figure 6.

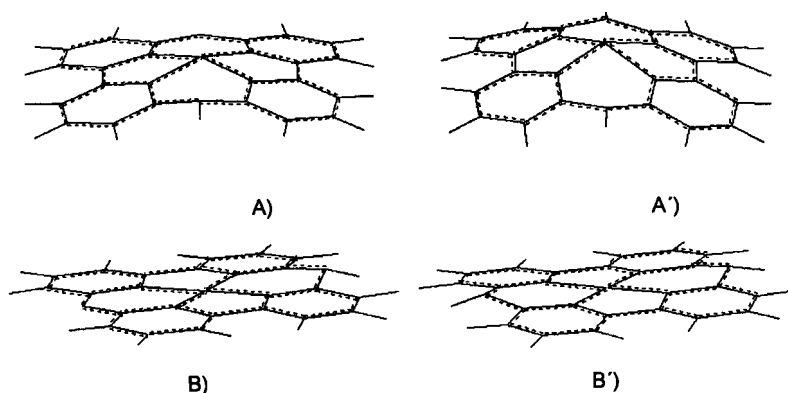


FIGURE 5 Monoprotonated (A,B) and diprotonated (A',B') structures used to model a protic environment for Zn (A) and Ni (B) complexes. Bent structures result from either PM3 or AM1 calculations. PM3 results shown.

## UV-vis Spectroscopy

### *Bis-azabipy Ligands*

The UV-vis spectrum of the macrocyclic ligand is largely dependent on the characteristics of the solvent, showing a band structure in the low energy region that only develops in non-protic environments (Fig. 7). This behavior has been previously explained on the basis of an amine-imine tautomeric equilibrium [29–31, 38]. The fully conjugated imine form, stable in non protic solvents, was supposed to be responsible of the low energy features, which disappear in protic media where the amine form becomes stabilized. However, when an isolated molecule is considered, no bands in the low energy region are predicted by the ZINDO/S-CI calculations regardless of the planarity of the system or the tautomeric form under study.

#### *(a) Aprotic Environment*

When a single ligand molecule is used to model the system in a non-protic medium the spectrum of Table I, 3rd column is calculated. No bands result for energies lower than 420 nm, rendering no interpretation, therefore, to the low energy experimental features around 400–500 nm (Fig. 7b). Analysis of the assignments shows that the bands originate in electronic excitations from  $\pi$  orbitals, mainly centered on the aza N but delocalized in the  $\pi$ -system, to fully delocalized  $\pi$  orbitals, namely  $N \rightarrow \pi^*$  transitions. From these data, it can be inferred that a more extended delocalized  $\pi$  system should

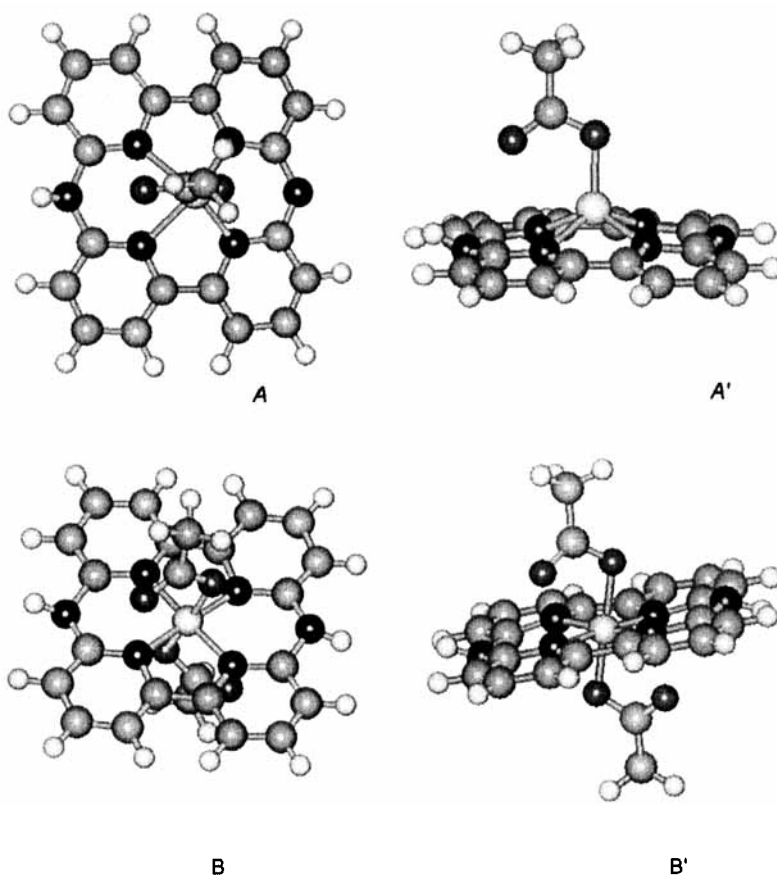


FIGURE 6 Example of the structures used to model the influence of the environment (acetic acid) by means of coordination of the counterion, as result from PM3 calculations. Single-coordination in the Zn complex in upper view; (A) and side view; (A') bi coordination in the Ni complex in upper view; (B) and side view; (B'). Single coordination has also been considered in the Ni calculations.

be capable of decreasing the calculated energy of the transitions. We have modeled, thence, our system, by means of two ligand molecules, in a parallel arrangement (see Fig. 3a) that allows their mutual stabilization by  $\pi$ -interactions. Table I (column 1) shows the calculated electronic transition bands in the UV-visible region for our model system. They are compared (column 5) with the experimental bands for the bis-azabipy ligand in chloroform. The comparative analysis of the spectra demonstrate the feasibility of the model. The assignment of the transitions does not change, relative to the monomers, but the  $\pi$ -orbitals involved are delocalized over

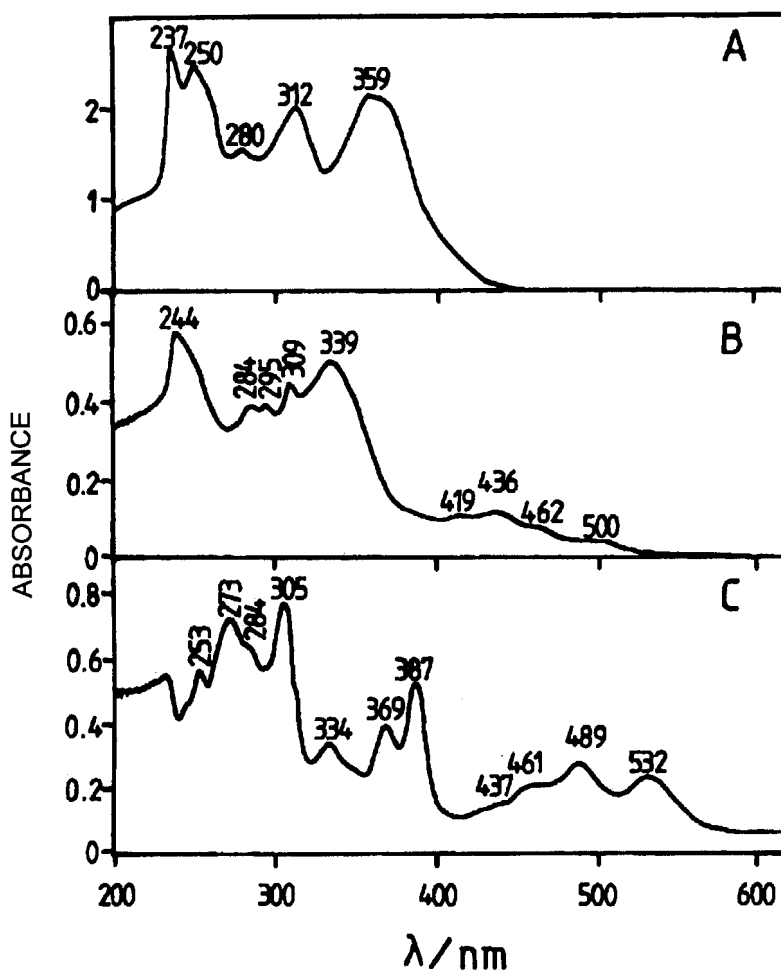


FIGURE 7 UV-vis spectra for: (A) bis-azabipyridyl ligand  $1.32 \times 10^{-4}$  M in dil acetic acid; (B) bis-azabipyridyl ligand  $3.28 \times 10^{-5}$  M in  $\text{CHCl}_3$ ; and (C) Ni-bis-azabipyridyl complex  $1.27 \times 10^{-4}$  M in  $\text{CHCl}_3$ .

the entire dimeric system. The distance between the moieties that provides best fitting of the ZINDO/S-CI calculated spectrum to the experimental data correspond to an interplanar separation of  $3.3 \text{ \AA}$  between the monomers, for the PM3 stabilized planar structure. Distances ranging from  $3.0 \text{ \AA}$  to  $4.3 \text{ \AA}$  have been compared for the PM3 and the AM1 derived structures.

TABLE I Bis-azabipy ligand  $3.28 \times 10^{-5}$  M in chloroform. Observed and calculated electronic transition bands<sup>(a)</sup>

$E_{calc}^{(b)(d)}$	$Osc.Str^{(b)}$	$E_{calc}^{(c)(d)}$	$Osc.Str^{(c)}$	$E_{exp}^{(e)}$
504.1	.0000			500 (1200)
463.6	.0275			462 (2300)
439.1	.0055			436 (3400)
417.6	.0940	423.6	.0000	419 (3100)
368.5	.0126			419
354.5	.3603	364.5	.9200	339 (15200)
351.6	.6863	333.7	.6403	339
338.8	.0001	318.6	.0000	
337.7	.8671	314.7	.0000	339
333.3	.0146			
308.1	.2522	304.3	.5561	309 (13400)
306.3	.0124			309
305.7	.0231			309
299.1	.0150			
297.7	.3956	275.1	.1448	295 (11600)
293.5	.0267			295
292.8	.4627			295
277.1	.2000			284 (11600)
275.1	.1488			284
270.8	.4199			284
262.8	.7026	259.4	.2510	241 (17400)

(a) Values in nm.

(b) Dimeric structure (Fig. 3a).

(c) Monomeric structure (Fig. 2b).

(d) See text for assignments.

(e) (e), Molar extinction coefficient,  $L \cdot cm^{-1} \cdot mol^{-1}$ .**(b) Protic Environment**

Table II shows the observed electronic transition bands in the UV-visible region for  $1.32 \times 10^{-4}$  M bis-azabipy in acetic acid, compared with the calculated bands for the system defined by a single molecule modeled in protic media (Figs. 1.b and b'). Absorption bands start to develop in the 400 nm region associated with electronic excitations from  $\pi$ -orbitals, mainly centered on the aza N but delocalized in the  $\pi$ -system, to fully delocalized  $\pi$ -orbitals ( $N \rightarrow \pi^*$ ). The agreement between experimental and calculated spectra is remarkable. This evaluation is based on the consideration that some bands, as the lowest energy one, calculated as Laporte forbidden, can gain intensity through vibronic coupling. The bands of highest intensity, in the high energy region, are built up from several calculated contributions, that should be added to reproduce the intensity of the peak. Double excitations, which are probably induced in this region are not included in the calculation, rendering, however, a peak of lower intensity than the

TABLE II Bis-azabipy ligand  $1.32 \times 10^{-4}$  M in 5% v/v acetic acid (Fig. 4b) observed and calculated electronic transition bands<sup>(a)</sup>

$E_{calc}^{(b)}$	Osc.Str.	$E_{exp}^{(c)}$
409.9	.0000	412
355.0	.9900	359(16200)
312.5	.6300	312(15200)
288.0	.0060	
283.9	.0130	280(11500)
280.3	.0000	
273.2	.0130	
267.1	.1450	250(18800)
266.2	.0010	250
260.2	.2000	250
260.1	.1200	250
241.3	.2000	237(20100)
241.5	.1100	237

<sup>(a)</sup> Values in nm.

<sup>(b)</sup> See text for assignments.

<sup>(c)</sup> ( $\epsilon$ ), Molar extinction coefficient,  $L \cdot cm^{-1} \cdot mol^{-1}$ .

experimental one. This analysis holds for all the systems. Protonation of the macrocycles decreases the electronic delocalization and destroys the stability of the dimers, a fact that is reflected in the lack of bands in the low energy region of the spectrum (Fig. 7a) and in the feasibility of its interpretation by monomeric models.

### Zn(II) and Ni(II) Complexes

The influence of the environment also becomes evident for the Zn(II)- and Ni(II)-bis-azabipyridyl complexes. A band structure develops in both cases, in the low energy region, in aprotic (Fig. 7c), but not in protic solvents (Fig. 8).

#### (a) Aprotic Environment

When the Zn complex is considered in an aprotic environment, the low energy region can only be reproduced when a dimeric model is used for the calculations (with the monomers separated  $3.8 \text{ \AA}$ ). Results are shown in Table III (column 1) in comparison with the experimental data (column 5). Data for the monomeric model fail to reproduce the low energy region. Because of the stability of the  $d^{10}$  closed-shell, the  $d$  orbitals of Zn(II) lie very low in energy and are, therefore, not involved in transitions. The transitions are calculated, as in the case of the ligand, to arise from electron promotions

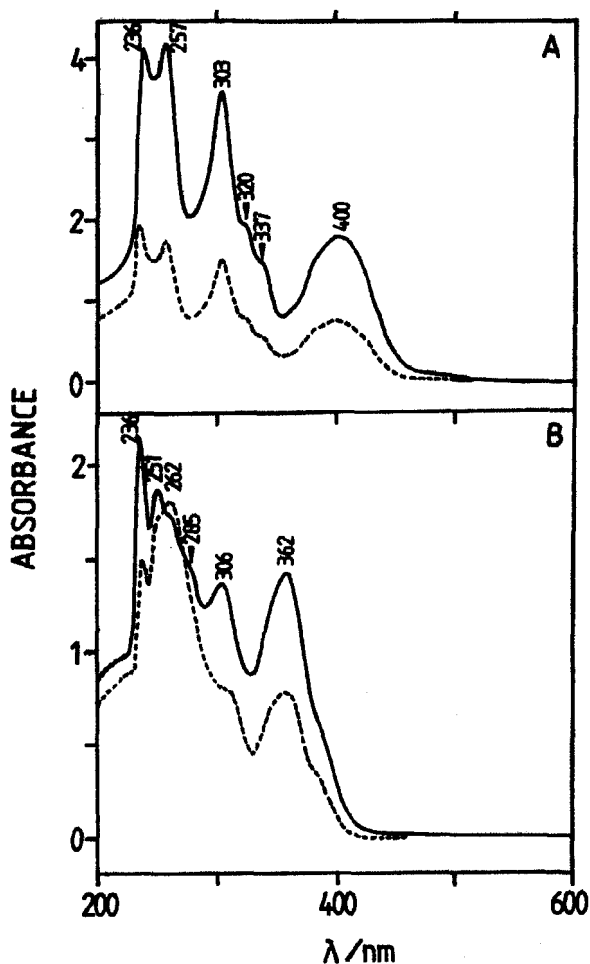


FIGURE 8 UV-vis spectra in dil 5% acetic acid for: (A) Ni-bis-azabipyridyl complex:  $1.9 \times 10^{-4}$  M (solid line),  $7.1 \times 10^{-5}$  M (dashed line); (B) Zn-bis-azabipyridyl complex:  $1.2 \times 10^{-4}$  M (solid line),  $6.0 \times 10^{-5}$  M (dashed line).

from  $\pi$ -orbitals mainly centered on the aza nitrogens (N) to  $\pi^*$  ( $N \rightarrow \pi^*$ ) delocalized over the aromatic system.

The Ni complex is the unique case for which low energy bands are calculated even when a monomeric structure is considered (Tab. IV, column 1). They are associated, in the monomer, to  $d \rightarrow d$  transitions. However, the best agreement with experiment is attained when calculations are based on a dimeric model, with an interplanar separation of  $3.4 \text{ \AA}$  (Tab. IV). For this model,  $d \rightarrow d$  and  $N \rightarrow \pi^*$  transitions share the low energy region (N stands



TABLE III Zinc-bis-azabipy complex in chloroform<sup>(a)</sup>. Observed and calculated electronic transition bands<sup>(b)</sup>

$E_{calc}$ <sup>(c)(e)</sup>	<i>Osc.Str.</i> <sup>(c)</sup>	$E_{calc}$ <sup>(d)(e)</sup>	<i>Osc.Str.</i> <sup>(d)</sup>	$E_{exp}$
556.6	.0000			
540.8	.0045			520
464.7	.0046			467
445.4	.0000			
430.5	.0011	440.2	.0000	424
417.1	.0000			
381.8	.0006			
367.8	1.1265	370.7	.7341	375
349.6	.9409	352.8	1.0409	340
349.5	.1138	324.5	.0000	340
342.8	.0011	318.7	.0082	
338.8	.0001			
337.5	.0000			
326.5	.0381			
324.5	.0000			
320.5	.0214			
316.7	.0008			
310.9	.0007			
310.5	.5154	305.1	.3284	310
308.2	.0000	301.5	.0000	
303.3	.3013	286.2	.0000	290
301.5	.0000	273.9	.0010	
297.5	.0000	269.9	.3740	
293.5	.0000			
292.5	.0000			
290.7	.0001			
290.3	.0034			
286.7	.0084			
286.0	.0000			
283.0	.0053			
281.9	.1493			
275.3	.3900			

<sup>(a)</sup> Saturated solutions, ca.  $10^{-5}$  M.

<sup>(b)</sup> Values in nm.

<sup>(c)</sup> Dimeric structure (Fig. 3c).

<sup>(d)</sup> Monomeric structure- not shown, correspond to one moiety of Figure 3c.

<sup>(e)</sup> See text for assignments.

for the same orbital type previously described for the Zn complexes). Nevertheless, only the latter are necessary for an appropriate assignment of the experimental features. We associate to them, which gain intensity through vibronic coupling, the origin of the bands around 500 nm (Fig. 7).

### (b) Protic Environment

A protic environment modifies in a similar manner the UV-vis spectra of both metal complexes. The modification pattern is associated with the band structure in the low energy region, which disappears in acid media. At the

TABLE IV Nickel-bis-azabipy complex  $1.27 \times 10^{-4}$  M in chloroform. Observed and calculated electronic transition bands<sup>(a)</sup>

$E_{calc}^{(b)}$	$Osc.Str.^{(b)}$	$E_{calc}^{(c)}$	$Osc.Str.^{(c)}$	$E_{exp}^{(d)}$	$Assignment^{(b)}$
525.3	.0000	510.7	.0000	532(1800)	$N \rightarrow \pi^*$
506.8	.0000				$d \rightarrow d$
501.1	.0000				$d \rightarrow d$
496.0	.0000				$d \rightarrow d$
495.9	.0000				$d \rightarrow d$
480.5	.0000	496.0	.0000	489(2200)	$N \rightarrow \pi^*$
461.2	.0000	463.4	.0000	461(1700)	$N \rightarrow \pi^*$
456.9	.0000	459.5	.0000		$d \rightarrow d$
456.8	.0000	403.4	.0000		$d \rightarrow d$
435.9	.0000			437(1300)	$N \rightarrow \pi^*$
397.9	.0000				$d \rightarrow d$
397.9	.0000	390.9	.6494		$d \rightarrow d$
382.6	.0000				$d \rightarrow d$
380.6	1.0144			387(4100)	$N \rightarrow \pi^*$
376.3	.0002	376.2	.7331		
359.6	1.0573			369(3100)	$N \rightarrow \pi^*$
352.5	.0000				
348.8	.0144	332.1	.0000	334(2600)	$N \rightarrow \pi^*$
312.1	.2315	322.7	.0000	305(6000)	$N \rightarrow \pi^*$
311.7	.0007	311.1	.1315		
308.1	.0034			284(5000)	$N \rightarrow \pi^*$
287.3	.0034				
283.9	.0005				
280.1	.0101	279.3	.2794		
277.6	.0000	272.8	.0401		
276.9	.0000	271.7	.3947		
276.7	.0107			273(5500)	$N \rightarrow \pi^*$
274.5	.5395			273	$N \rightarrow \pi^*$
273.2	.1868			273	$N \rightarrow \pi^*$
270.1	.0000				$N \rightarrow \pi^*$
269.2	.2842	267.1	.0513	273	$N \rightarrow \pi^*$
268.8	.0000	263.8	.2720		$N \rightarrow \pi^*$
268.6	.0755	245.7	.2575	273	$N \rightarrow \pi^*$

<sup>(a)</sup> Values in nm.<sup>(b)</sup> Dimeric structure (Fig. 3b).<sup>(c)</sup> Monomeric structure- not shown, correspond to one moiety of Figure 3b.<sup>(d)</sup> ( $\epsilon$ ), Molar extinction coefficient,  $L \cdot cm^{-1} \cdot mol^{-1}$ .

same time, a broad feature around 400 nm develops (Fig. 8). Higher concentrations of complex increase the height of the 400 nm peak relative to the bands in the high energy region, an effect that becomes more notorious in the Zn macrocycle. The bands in the high energy region, on the other hand, show better resolution.

Different models have been compared in their ability to reproduce the UV-vis spectra in acid media.

On the basis of the results previously found for the ligand, the Zn-bis-azabipyridyl complex has been first modeled, in protic media, as positive structures protonated on either one or both aza-nitrogens (Fig. 5). However,

none of these models is capable of reproducing the features of the experimental spectrum in relation to the absence of bands at energies lower than 400 nm. (Tab. V, columns 3,4). An intense band is calculated at 444 nm, with no experimental counterpart. Considering that the protonated structures are stabilized as acetate anions during the synthetic paths, the specific coordination of one or two acetates with the central metal atom has been modeled (Fig. 6). By means of this coordination the anionic species counterbalance the positive charge localized on the metal center, which is calculated, within a Mulliken population analysis, as 0.68 or 0.25 au at the AM1 or ZINDO/S levels, respectively. When a model with one coordinated anion is used for the calculations, the comparison of the experimental and the calculated spectra of Zn-bis-azabipyridyl (Tab. V, columns 1,2) relates the bands at 380 and 339 nm to the experimental feature at 362, which is not resolved but appears as a broad band with a shoulder. Calculated features in the low energy region are in good agreement with the experimental ones. Due to the electronic configuration of Zn(II), transitions do not involve  $d$  orbitals, but are originated, as shown in the table, in  $N \rightarrow \pi^*$  excitations.

It has been experimentally found that higher concentrations of complex (Fig. 8) result in an increasing intensity of the peak at 362 nm. In the high energy region, on the other hand, the broad signal at 262 nm decreases and is resolved in one feature at 251 nm with shoulders at 262 and 285 nm. Our model certainly reproduces the effect of high concentrations of complex (Tab. V). The spectrum for lower concentrations is not easily reproduced. Diprotonated models with two coordinated acetate anions fail to give the

TABLE V Zinc-bis-azabipy complex in acetic acid. Observed and calculated electronic transition bands<sup>(a)</sup>

$E_{calc}^{(b)}$	$Osc.Str.^{(b)}$	$E_{calc}^{(c)}$	$Osc.Str.^{(c)}$	$E_{exp}^{(d)}$	Assignment
422	0.006				$N \rightarrow \pi^*$
383	0.416	444	0.261	362	$N \rightarrow \pi^*$
339	0.582	349	0.582	362	$N \rightarrow \pi^*$
328	0.035	331	0.250		$N \rightarrow \pi^*$
307	0.102			306	$N \rightarrow \pi^*$
301	0.109	321	0.421	306	$N \rightarrow \pi^*$
290	0.052				$N \rightarrow \pi^*$
285	0.297	297	0.159	285	$N \rightarrow \pi^*$
268	0.223	260	0.131	262	$N \rightarrow \pi^*$
246	0.332	249	0.332	251	$N \rightarrow \pi^*$
240	0.251	237	0.151	236	$N \rightarrow \pi^*$

<sup>(a)</sup> values in nm.

<sup>(b)</sup> Protic media modeled by means of the explicit definition of the acetate anion coordinated to the metal center together with monoprotation of an aza nitrogen (Fig. 6a).

<sup>(c)</sup> Protic media modeled by means of monoprotation of a aza nitrogen (Fig. 5a).

<sup>(d)</sup> From Figure 8b.

experimental features (data not shown). The effect of concentration seems to be mainly related to the intensity of the peaks, and may imply the contribution of more than one species in equilibrium. This will be further discussed for the Ni case.

The same models have been compared for the Ni-bis-azabipyridyl complex. Instead of following the same pattern, the specific coordination of the acetate anion does not accurately reproduce, in this case, the experimental spectrum. The transitions calculated with this model, which develop in the low energy region, *i.e.*, between 550 and 400 nm, do not correlate with experience (Tab. VI, columns 1, 2). Having its maximum at 400 nm, the calculated bands are mainly associated with excitations from a bonding Ni—O orbital to the  $\pi$  delocalized system. There is also a lack of precision in the reproduction of the bands in the high energy region, where features are calculated with no experimental counterpart.

The spectrum is more accurately reproduced when a monoprotonated complex, with no counterion specifically defined, is used for the calculations

TABLE VI Nickel-bis-azabipy complex in acetic acid. Observed and calculated electronic transition bands<sup>(a)</sup>

$E_{calc}^{(b)}$	$Osc.Str.^{(b)}$	$E_{calc}^{(c)}$	$Osc.Str.^{(c)}$	$E_{exp}^{(d)}$	Assignment
760	0.000				d → d
559	0.013				N → $\pi^*$
536	0.001				d → d
485	0.002	481	0.002	483 <sup>(f)</sup>	N → $\pi^*$
470	0.007				d → d*
449	0.040	447	0.037		d → $\pi^*$
415	0.191	394	0.519	400	d → $\pi^*$
401	0.094			400	N → $\pi^*$
375	0.119	352	0.365	352 <sup>(e)</sup>	d → $\pi^*$
356	0.121				N → $\pi^*$
343	0.265	323	0.009	337	d → $\pi^*$
311	0.154	308	0.010	320	N → $\pi^*/d \rightarrow \pi^*$
290	0.342	306	0.082	320	N → $\pi^*/\pi \rightarrow \pi^*$
		304	0.107	303	d → $\pi^*$
		292	0.270	303	$\pi \rightarrow \pi^*$
270	0.386				d → $\pi^*$
262	0.136	263	0.129	257	$\pi \rightarrow \pi^*$
258	0.189	255	0.520	257	$\pi \rightarrow \pi^*$
247	0.290				d → $\pi^*$
233	0.270	238	0.444	236	d → $\pi^*$
228	0.369				d → $\pi^*$

<sup>(a)</sup> Values in nm.

<sup>(b)</sup> Protic media modeled by means of the explicit definition of the counteranion coordinated with the metal center together with monoprotonation of a aza nitrogen (Fig. 6a).

<sup>(c)</sup> Protic media modeled by means of monoprotonation of a aza nitrogen (Fig. 5b).

<sup>(d)</sup> From Figure 8a.

<sup>(e)</sup> Hidden under the broad feature at 400 nm.

<sup>(f)</sup> Very low intensity, observed only in concentrated solutions.

(Tab. VI, columns 3,4). The presence of the counterion is certainly important in determining the stabilization of single charged species, but the interactions are not always strong enough to allow the definition of coordinated "molecules" as those shown in Figure 6. For this model system, the calculated intensity of the band at 400 nm is larger than the one experimentally measured, but the dependence of the relative intensities on the concentration has to be considered in the interpretation. Moreover, slight structural modifications that influence the symmetry of the molecule are reflected in the calculated intensity, as it is based on the consideration of selection rules within group theory. In addition to the band at 400 nm, another one is calculated at 352 nm, which is hidden under the broad feature of the experimental spectrum. The other calculated bands, which certainly correlate with the experimental features, are shown in Table VI, together with the assignments. In relation to the relative intensities of the bands in the low and high energy regions, one has to remember that double excitations, which can contribute to the high energy transitions, are not included in the calculations. As a way of testing the reliability of the calculations, the 480 nm region of the spectrum has been zoomed, and a very weak band 483 nm was observed.

A Mulliken population analysis of the Ni complex does not render the same positive charge on the metal center as for the Zn structure. This fact supports the different degree of influence of the counterions, through coordination, in both cases. Further justification can be found in the ligand field stabilization of square planar complexes of Ni(II).

## CONCLUSIONS

We have examined the structural characteristics of a bis-azabipyridyl macrocycle and its Zn(II) and Ni(II) complexes, focusing our attention on the influence of the environment. Within a discrete model, coordinated "solvent molecules" (protons, counterions or a second monomer) have been simulated.

The most conclusive data are those that follow from the reproduction and theoretical assignment of the experimental UV-vis transitions, for which the low energy region largely depends on the structural and electronic characteristics of the species under consideration.

According to the results of ZINDO/S-CI calculations, and to the assignments of the low energy bands, both the ligands, as well as the Zn(II) and Ni(II) complexes are stabilized by  $\pi$ -stacking interactions in aprotic

solvents. Protic solvents decrease the electronic delocalization through direct coordination, an effect that is mainly related to the protonation of the aza-nitrogens. Whereas diprotonation occurs for the ligands, the influence of the counterions stabilizes single protonation of the complexes. Coordination of the counterion is certainly defined for the Zn(II) complex but not for the Ni(II) complex, a fact that is justified by the different calculated charge densities on both metal centers.

The calculations have demonstrated the applicability of ZINDO/S-CI methodologies to study the structural and electronic characteristics of complex systems, and its capability to analyze the influence of different environments.

### Acknowledgements

This work has been financed by the Consejo Nacional de Investigaciones Científicas y Técnicas (CONICET), the Universidad Nacional de La Plata (Argentina), FONDECYT (Chile), project N° 1000746 and Universidad de Santiago de Chile, project DICYT N° 9942CM. GLE is a member of the research staff of CONICET (República Argentina).

### References

- [1] J. D. Bernal and F. D. Fowler, *J. Chem. Phys.* **1**, 515 (1933).
- [2] C. J. Cramer and D. G. Truhlar, *Continuum Solvation Models: Classical and Quantum Solvation Implementations in Reviews in Computational Chemistry*; K. B. Lipkowitz and D. B. Boyd (Eds.), Vol. 6, VCH Publishers, New York, 1995, Chapter 1.
- [3] W. N. Olmstead and J. I. Brauman, *J. Am. Chem. Soc.* **99**, 4219 (1977).
- [4] J. Chandrasekhar, S. F. Smith and W. L. Jorgensen, *J. Am. Chem. Soc.* **107**, 154 (1985).
- [5] M. Karelson and M. C. Zerner, *J. Am. Chem. Soc.* **112**, 9405 (1990).
- [6] A. H. de Vries, P. Th. van Duijnen and A. H. Juffre, *Int. J. Quantum Chem., Quantum Chem. Symp.* **27**, 451 (1993).
- [7] V. Luzhkov and A. Warshel, *J. Comp. Chem.* **13**, 199 (1992).
- [8] K. K. Stavrev and M. C. Zerner, *J. Am. Chem. Soc.* **117**, 8684 (1995).
- [9] U. C. Singh and P. A. Kollman, *J. Comp. Chem.* **7**, 718 (1986).
- [10] A. Broo, G. Pearl and M. C. Zerner, *J. Phys. Chem. A* **101**, 2478 (1997).
- [11] G. Pearl and M. C. Zerner, *J. Am. Chem. Soc.* **121**, 399 (1999).
- [12] F. Maseras and K. Morokuma, *J. Comp. Chem.* **16**, 1170 (1995).
- [13] M. Svensson, S. Humbel, R. J. Froese, T. Matsubara, S. Sieber and K. Morokuma, *J. Phys. Chem.* **100**, 19357 (1996).
- [14] F. M. Hornung, F. Baumann, W. Kaim, J. A. Olabe, L. Slep and J. Fiedler, *Inorg. Chem.* **37**, 311 (1998).
- [15] B. S. Brunschwig, C. Creutz and N. Sutin, *Coord. Chem. Rev.* **177**, 61 (1998).
- [16] Y. K. Shin, D. J. Szalda, B. S. Brunschwig, C. Creutz and N. Sutin, *Inorg. Chem.* **36**, 3190 (1997).
- [17] Y. K. Shin, B. S. Brunschwig, C. Creutz, M. D. Newton and N. Sutin, *J. Phys. Chem.* **100**, 1104 (1996).

- [18] A. Parise, J. Olabe and G. Estiú, unpublished results.
- [19] J. Ridley and M. C. Zerner *Theor. Chim. Acta* **32**, 111 (1973).
- [20] J. Ridley and M. C. Zerner, *Theor. Chim. Acta* **42**, 223 (1976).
- [21] M. C. Zerner, ZINDO Package. *Quantum Theory Project*, University of Florida, Gainesville, USA.
- [22] B. R. Eggins and J. McNeil, *J. Electroanal. Chem.* **148**, 17 (1983).
- [23] I. Taniguchi, In: *Modern Aspects of Electrochemistry* J. O'M. Bockris, E. White and B. E. Conway (Eds.), p. 327, Plenum Press, New York (1989).
- [24] J. P. Sauvage, *J. Am. Chem. Soc.* **108**, 7461 (1986).
- [25] J. J. P. Stewart, Mopac, version 7.0. F. J. Seiler Research Laboratory, United States Air Force Academy, CO 80840, USA, 1994.
- [26] M. C. Zerner, Semiempirical Molecular Orbital Methods, In: *Reviews in Computational Chemistry* K. B. Lipkowitz and D. B. Boyd (Eds.), Vol. 2, VCH Publishers, New York, 1991, Chapter 8.
- [27] M. G. Cory, and M. C. Zerner, *Chem. Rev.* **91**, 813 (1991).
- [28] J. Canales, J. Ramirez, G. Estiu and J. Costamagna, *Polyhedron*, **19**, 2373 (2000).
- [29] S. Ogawa, *J. Chem. Soc. Perkin I* p. 214 (1977).
- [30] S. Ogawa, T. Yamaguchi and N. Gotoh, *J. Chem. Soc. Perkin I* p. 976 (1974).
- [31] S. Ogawa, T. Yamaguchi and N. Gotoh, *J. Chem. Soc. Chem. Comm.* p. 577 (1972).
- [32] W. Saenger, *Principles in Nucleic Acid Structure*; Springer-Verlag: New York, 1984.
- [33] (a) T. Blundel, J. Singh, J. Thornton, S. K. Burley, G. A. Petsko, *Science* **234**, 1005 (1986); (b) S. K. Burley, G. A. Petsko, *Adv. Protein Chem.* **39**, 125 (1988); (c) C. A. Hunter, J. Singh, J. Thornton, *J. Mol. Biol.* **218**, 837 (1991).
- [34] M. J. Stillman, In: "*Phthalocyanines, Properties and Applications*", C. C. Leznof and A. B. P. Lever (Eds.), VCH, New York, 1993, Chp. 5.
- [35] (a) C. Chipot, R. Jaffe, B. Maigret, D. A. Pearlman and P. A. Kollman, *J. Am. Chem. Soc.* **118**, 11217 (1996); (b) Z. Wang, T. Hirose, K. Hiratani, Y. Yang and K. Kasuga, *Chemistry Letters* p. 603 (1996).
- [36] G. L. Estiu and M. C. Zerner, *J. Am. Chem. Soc.* **121**, 1893 (1999).
- [37] G. L. Estiu and M. C. Zerner, *J. Phys. Chem.* **99**, 13819 (1995).
- [38] S. Ogawa and S. Shiraishi, *J. Chem. Soc. Perkin I* p. 2527 (1980).